JOURNAL OF AGRICULTURAL AND FOOD CHEMISTRY
ARTICLE

J. Agric. Food Chem. 2010, 58, 3407–3414 3407
DOI:10.1021/jf904401j

Modeling Relationships among Active Components in Black Raspberry (*Rubus occidentalis* L.) Fruit Extracts Using High-Resolution ^{1}H Nuclear Magnetic Resonance (NMR) Spectroscopy and Multivariate Statistical Analysis

Faith J. Wyzgoski,*,† Liladhar Paudel,‡ Peter L. Rinaldi,‡ R. Neil Reese,§ Mustafa Ozgen,∥,⊥ Artemio Z. Tulio, Jr.,⊥ A. Raymond Miller,⊥ Joseph C. Scheerens,⊥ and James K. Hardy‡

†Department of Chemistry, The Ohio State University—Mansfield, 1760 University Drive, Mansfield, Ohio 44906, ‡Department of Chemistry, University of Akron, Akron, Ohio 44325-3601, §Department of Biology and Microbiology, South Dakota State University, Brookings, South Dakota 57007, ∥Department of Horticulture, Gaziosmanpaşa University, Tasliciftlik, Tokat 60240, Turkey, and ⊥Department of Horticulture and Crop Science, The Ohio State University, Ohio Agricultural Research and Development Center, 1680 Madison Avenue, Wooster, Ohio 44691

A process was developed to ascertain the bioactive components of black raspberry (*Rubus occidentalis* L.) fruit extracts by relating chemical constituents determined by high-field nuclear magnetic resonance (NMR) spectroscopy to biological responses using partial least-squares regression analysis. To validate our approach, we outlined relationships between phenolic signals in NMR spectra and chemical data for total monomeric anthocyanin (TMA) content and antioxidant capacity by the ferric-reducing antioxidant power (FRAP) and 2,2-diphenyl-1-picrylhydrazyl (DPPH) assays. Anthocyanins, cyanidin 3-*O*-rutinoside (Cy 3-rut), cyanidin 3-*O*-(2(G))-xylosylrutinoside (Cy 3-xylrut), and cyanidin 3-*O*-glucoside (Cy 3-glc), were significant contributors to the variability in assay results, with the two most important NMR bins corresponding to the methyl peaks in Cy 3-rut (6‴) and/or Cy 3-xylrut (6^{IV}). Many statistically important bins were common among assay models, but differences in structure−activity relationships resulted in changes in bin ranking. The specificity of these results supported the application of the process to investigate relationships among health-beneficial natural products and potential biological activity.

KEYWORDS: Black raspberry; chemoprevention; anthocyanins; cyanidin 3-glucoside; cyanidin 3-rutinoside; cyanidin 3-xylosylrutinoside; metabolomics; NMR; chemometrics

INTRODUCTION

Metabolomics provides a powerful approach to identify potentially useful compounds from plants by profiling the entire metabolome or specific fractions prior to determining biological or chemical activity (*1*, *2*). The metabolites are chemically characterized, and the variation in their concentrations is measured. Those compounds playing key roles in observed physiological variation or specific bioassays are then identified using statistical analyses (e.g., principal component and/or partial least-squares analysis). Such metabolomic approaches avoid problems with additive or synergistic effects by recognizing all of the components that may be involved in the assay and then relying on the statistical analysis of the data to determine which compounds control the observed phenomenon. This approach is gaining more prominence in studies of plants, wine, and food products (*3*−*6*).

*To whom correspondence should be addressed. Telephone: 419-755-4342. E-mail: wyzgoski.1@osu.edu.

Our research uses ^{1}H nuclear magnetic resonance (NMR) data from minimally purified black raspberry (BR) (*Rubus occidentalis* L.) extracts and multivariate statistical analysis in a more efficient modeling process that can relate a biological or chemical response to the important berry constituents that drive it prior to chemical identification of all metabolites. This approach takes advantage of genetically and environmentally induced variation in secondary product complements to elucidate the additive and synergistic effects of specific compounds. Once spectral regions responsible for these relationships are identified by the model, compound structures can be verified using 2D NMR methods, such as heteronuclear single-quantum correlation (HSQC) (*7*) and heteronuclear multiple-bond correlation (HMBC) (*8*) experiments.

BR extracts were chosen for the development of the analytical model systems for several reasons. Recent clinical research with animal/human models and subjects provides compelling evidence that BRs contain secondary products that have chemopreventive properties with regard to oral, esophageal, and colon cancers (*9*−*21*), including angiogenesis inhibitors (*22*). Mediation of apoptosis on cancer cell lines has also been reported in a recent

Published on Web 03/01/2010

study with Korean BR *Rubus coreanus* Miq. (*23*). Additionally, we have developed a significant database of BR phenolic constituents especially with regard to the primary role of anthocyanin constituents in the antioxidant capacity of this species (*24*−*28*). Moreover, because product source, fruit maturation, and postharvest storage conditions significantly influence BR phytonutrient content (*24*−*26*), we can easily obtain fruit samples of variable antioxidant capacity and phenolic profiles as needed for metabolomic model development.

Our understanding of the phenolic constituents and antioxidant properties of BRs provides an opportunity to validate our approach and to refine various model parameters using relatively simple chemical assays before they are applied to the more complex biological systems. These assays included total monomeric anthocyanin (TMA) (*29*), a commonly used pH differential method with spectrophotometric detection, and two different antioxidant capacity measurements, one relying on single-electron transfer [i.e., ferric-reducing antioxidant power (FRAP) (*30*)] and the other involving the scavenging of the radical 2,2-diphenyl-1-picrylhydrazyl [(i.e., DPPH) (*31*)]. The purpose of this study was to test the power of our model by applying metabolomic techniques to determine interactivity among potentially bioactive components of BR using ^{1}H NMR spectra of 19 variable BR juice samples and partial least-squares (PLS) regression analysis against the dependent variables provided by assays of TMA, FRAP, and DPPH. In the process of achieving this goal and to optimize model building for identifying bioactive constituents in subsequent experiments, we employed commercially available metabolomic-based software to process the highly complex NMR spectra and to conduct statistical analyses relating binned NMR data with assay results.

MATERIALS AND METHODS

Materials. Caffeic acid, chlorogenic acid, quercetin dihydrate, quercetin 3-glucoside, gallic acid, ellagic acid, trifluoroacetic acid (TFA), 6-hydroxy-2,5,7,8-tetramethylchroman-2-carboxylic acid (trolox), 2,4,6-tris(2-pyridyl)-*s*-triazine (TPTZ), methanol-d_4 (99.8 atom % D), trifluoroacetic acid-*d* (99.5 atom % D), and tetramethylsilane were purchased from Sigma-Aldrich (St. Louis, MO). DPPH was purchased from EMD Biosciences, Inc. (San Diego, CA). Cyanidin 3-glucoside (Cy 3-glc), cyanidin 3-rutinoside (Cy 3-rut), and cyanidin 3-sambubioside (Cy 3-sam) were purchased as chloride salts from Polyphenols Laboratories AS (Sandnes, Norway). The C18 solid-phase extraction (SPE) and the C18 reverse-phase high-performance liquid chromatography (HPLC) analytical and guard columns were purchased from Alltech Associates, Inc. (Deerfield, IL).

Sample Acquisition and Analytical Preparations. A total of 19 fruit samples of 'Bristol', 'Jewel', 'Haut', or 'MacBlack' BRs were obtained from eight Ohio farms. Fruit samples were frozen on the farm after harvest and then transported on ice to the Ohio Agricultural Research and Development Center (OARDC). Before analysis, 100 g replicates of each fruit sample were thawed and then homogenized in a food-grade blender. From each of the resulting slurries, a juice sample for NMR spectroscopy was obtained by filtration through cheesecloth followed by centrifugation at 10000*g* for 15 min at 4 °C. In addition, for biochemical and HPLC analyses, 3 g aliquots of each slurry were transferred to a polypropylene tube and extracted for 1 h in 40 mL of an extraction buffer [70:29.5:0.5 (v/v/v) acetone, water, and acetic acid, respectively] commonly used to extract phenolic compounds (*32*). After vacuum filtration, acetone was removed by rotary evaporation and then the concentrated samples were brought to a final volume of 40 mL with distilled, deionized water.

Biochemical Analyses. All biochemical analyses were performed in duplicate for each crude extract. The antioxidant capacity was determined by the FRAP method of Benzie and Strain (*30*) and the free radical scavenging of DPPH by the method of Brand-Williams et al. (*31*), two methods that exhibited differing responses to BR in a previous study (*24*). For the FRAP analysis, an antioxidant reactant solution of 10 mM TPTZ and 20 mM ferric chloride was diluted in 300 mM sodium acetate buffer (pH 3.6) at a ratio of 1:1:10. To prepare the DPPH reactant solution, 40 mg/L of the radical were dissolved in 100% methanol. Assays were conducted by combining antioxidant reactants with 20 μL of individual crude extracts. Reactions were allowed to progress at 28 ± 2 °C for 30 min. Assay results were measured using a Beckman DU 640 spectrophotometer at 593 and 515 nm for FRAP and DPPH, respectively. For both antioxidant assays, trolox aliquots were thawed and used to develop a 10−100 μmol/L standard curve. All data were then expressed as trolox equivalents (TE, μmol).

The TMA contents of crude extracts were measured with a pH differential method described by Giusti and Wrolstad (*29*). The anthocyanin content of each duplicate was calculated using the molar absorptivity (ε) and molecular weight (MW) of Cy 3-rut (ε, 30 185; MW, 631.0) as described by Lohachoompol et al. (*33*).

Sample Preparation for NMR Analyses. BR juice samples for NMR examination were processed to remove free sugars by separation on C18 SPE columns. SPE columns were equilibrated with 25 mL of 0.1% TFA in double-distilled H_2O after column washing with 25 mL of 0.1% TFA in HPLC-grade methanol. Aliquots (4 mL) of BR juice, acidified by adding 0.1% TFA (v/v), were loaded onto individual columns and washed with an additional 25 mL of acidified water to remove free sugars. Anthocyanins and other phenolics were eluted with 25 mL of acidified methanol. Methanol was removed from the eluted materials under N_2 at 30 °C, and then water was removed by lyophilization. Dried samples were sealed under nitrogen gas in glass tubes capped with Teflon-lined caps and stored at −80 °C.

NMR Analyses. All NMR studies of BR extract samples were performed with a Varian INOVA 750 MHz NMR spectrometer (Varian, Inc., Palo Alto, CA) using a Varian triple-resonance ^{1}H{^{13}C/^{15}N} pulsed field gradient cryoprobe. Solid material (25−40 mg) derived from the column eluate was solubilized in a solution containing methanol-d_4/trifluouroacetic acid-*d* (95:5, v/v), and tetramethylsilane (TMS) was added as an internal chemical-shift reference standard. The samples were filtered through glass wool and placed in 5 mm NMR tubes. All samples were stored at 4 °C prior to analysis. The spectra were collected at 25 °C over a spectral width of 9830 Hz using a 7.5 μs (90°) pulse. The acquisition time was 2.7 s, and 128 transients were accumulated with presaturation of the HDO resonance at ca. 4.9 ppm. Data were processed with 0.5 Hz exponential line broadening and zero filled to 131 072 points before Fourier transformation.

Two-dimensional gradient assisted HSQC and HMBC NMR spectra were obtained at 25 °C with 90° pulse widths for ^{1}H and ^{13}C of 7.5 and 12.5 μs, respectively.

For the phase-sensitive HSQC spectra, the following conditions applied: acquisition time of 0.085 s, with ^{13}C WURST40 (*34*) decoupling, a relaxation delay of 1.0 s, polarization transfer delays Δ of 1.8 ms (based on $^1J_{CH}$ = 140 Hz), coherence selection gradients of 0.20 and 0.10 T/m with durations of 2.0 and 1.0 ms, respectively, and 16 transients averaged for each of 2 × 1024 free induction decays, in which t_1 was incremented to provide a spectral window of 38 666 Hz in the f_1 dimension, using the States method of phase-sensitive detection (*35*). The experiment time was ca. 10 h. Data were zero-filled to a 4096 × 8192 matrix and weighted with a sinebell function before Fourier transformation.

The HMBC spectra were obtained in a similar manner, except that the acquisition time was 0.122 s, 24 transients were averaged for each of 1024 increments, coherence selection gradients of 0.20 and 0.15 T/m with a duration of 2.0 ms each were applied, a fixed delay of 0.080 s was used to allow for the long-range heteronuclear anti-phase magnetization to develop from multiple-bond C−H couplings, and t_1 was incremented to provide a spectral window of 50 800 Hz in the f_1 dimension. Linear prediction was used to forward extend the data 2 times its original length. The data were zero-filled to an 8192 × 8192 matrix and weighted with a sinebell function before Fourier transformation. The experiment time was ca. 8 h. NMR spectra were compared to literature values (*36*−*38*) and those of pure standards when available to verify assignments.

Statistical Models for Compound Identification. ^{1}H NMR free induction decays (FIDs) were processed as a batch, using Bio-Rad's KnowItAll Metabolomics Software with a Lorentzian apodization of 0.3 Hz, baseline correcting with automatic base point detection and spline fitting, and referencing with the TMS peak set to 0 ppm. Alignment

macros were applied as a batch process to numerous specific locations along the spectrum to compensate for peak shifting because of pH and variation in the constituent concentrations among samples. Solvent (CD_3OD) peaks centered at 3.31 and at 3.35 ppm were flat-lined. Each spectrum was then normalized according to the peak area from 0.5 to 9.5 ppm.

Using the AnalyzeIt MVP application, prior to PLS, each spectrum was transformed by subtracting its baseline value and dividing by sample 2-norm (i.e., vector length normalization). Binning/bucketing was conducted using the IntelliBucket method, where the bin width was automatically adjusted on the basis of the overlap density heatmap (ODH) consensus spectrum and a bin width setting of 0.004 ± 0.002 ppm. The binning range was set from 0.5 to 9.5 ppm, excluding portions of the spectrum that had been presaturated at ~4.90 ppm and the regions that had been flat-lined. The matrices were then transferred to Infometrix Pirouette 4.0 software without preprocessing, and measurements for FRAP, TMA, and DPPH assays were added manually into the database for each sample.

A PLS regression analysis on the 19 BR extract samples was conducted using Pirouette. The peak intensities from 2153 bins for each sample were regressed against the assay results for TMA, FRAP, and DPPH, respectively. No preprocessing was conducted; the maximum number of factors was 18; and the probability threshold was 0.95. Orthogonal signal correction (OSC) (*39*) was used to remove components in our large X block that were orthogonal to the Y block, thus segregating the portion of the X block that was correlated. The regression vector values that were obtained with their corresponding regions for the bins from the NMR spectra were then ranked from highest to lowest.

RESULTS AND DISCUSSION

One-Dimensional NMR Analysis of Juice Samples. BR extracts contain complex mixtures of secondary plant products, but attempts to quantify the variability in phenolic compounds in raw juice samples by ^{1}H NMR spectroscopy are confounded by the large amount of free saccharides that produce resonances that dominate the spectra. Minimally purifying the BR extracts with C18 SPE columns to remove free sugars substantially enhanced spectral resolution, especially for the aromatic region (6−9.5 ppm), where protons of polyphenolics structures were observed. Resonances from the anthocyanins, Cy 3-glc, Cy 3-sam, cyanidin 3-xylosylrutinoside (Cy 3-xylrut), and Cy 3-rut (structures shown in **Figure 1**), the primary polyphenolic antioxidant constituents in BR fruit (*25*), can then be readily identified in the ^{1}H NMR spectra. Variations in chemical content become apparent when the spectra of different samples are compared (**Figure 2**). Resonances for pelargonidin 3-rutinoside (Pg 3-rut), a minor anthocyanin, containing a hydrogen atom at the 3′ position of its aglycone, can also be detected.

Integrated areas for proton 4 of the cyanidin/pelargonidin moieties, found in the 8.80−9.05 ppm region of the spectra, were used to quantify the relative differences in anthocyanin contents among the 19 BR samples. **Figure 3** shows the specific regions and how the peak areas and the corresponding anthocyanin contents differed for samples 12 and 19. An analysis of these regions (**Figure 4**) in all spectra revealed the 19 BR samples to be highly variable in anthocyanin content and in the ratio of the major BR anthocyanins, Cy 3-xylrut/Cy 3-rut. Anthocyanin contents and specifically levels of Cy 3-rut (HPLC detection) were previously reported to vary significantly among these BR samples from different producers (*28*). Correlation analyses indicated that TMA and Cy 3-rut variability among production locations could be attributed in part to environmental influences and differences in harvest and other production practices. Moreover, BR anthocyanin levels were found to fluctuate significantly just prior to and after peak ripeness (*24*) and during storage (*26*).

Spectral Alignment. The ^{1}H NMR spectra of the 19 BR samples were examined prior to statistical treatment of the data by PLS.

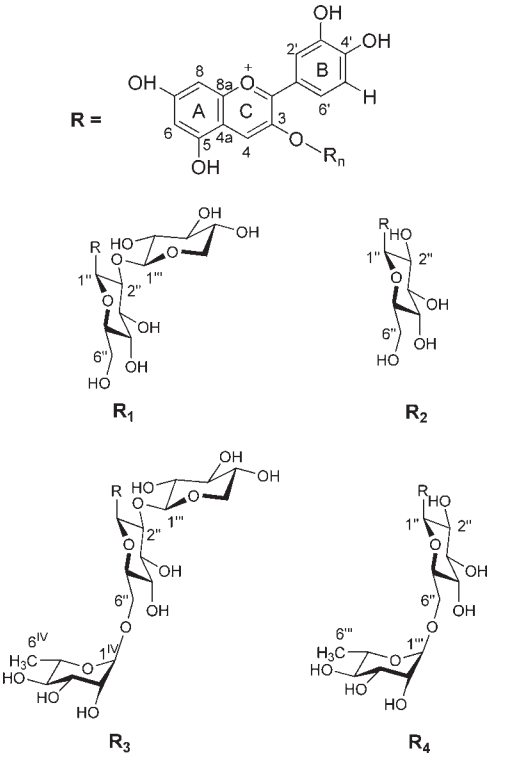

Figure 1. Basic structures of cyanidin and its glycosides in BRs: R_1, sambubioside; R_2, glucoside; R_3, xylosylrutinoside; and R_4, rutinoside.

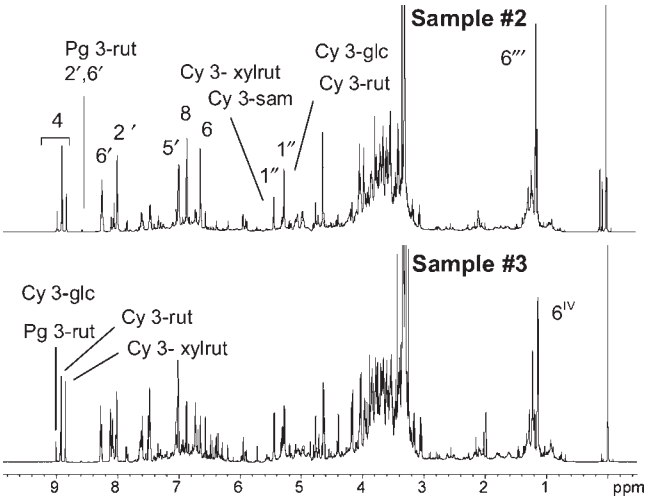

Figure 2. ^{1}H NMR spectra (750 MHz) showing proton assignments. Anthocyanin peaks that are identified include Cy 3-glc, Pg 3-rut, Cy 3-sam, Cy 3-rut, and Cy 3-xylrut.

Changes in chemical shifts were evident, and these were attributed to the variability in sample phenolic contents, differences in their relative concentration within samples, and the resulting variability in pH, occurring despite the addition of deuterated trifluoroacetic acid (TFA-*d*) to the sample solution. To resolve the chemical-shift differences, the spectra of all of the samples were overlapped and aligned at a number of specific peak regions using algorithms for local spectral alignment from Bio-Rad KnowItAll software. Anthocyanins are particularly sensitive to pH changes and subject to changes in chemical shifts, and illustrative of the alignment process, the resonances for H4 of the cyanidin moieties of three samples (1, 11, and 15) are shown before (**Figure 5A**) and after (**Figure 5B**) alignment in the 8.80−9.05 ppm regions of the

NMR spectra. Similar corrections were made for numerous peaks in each spectrum.

Statistical Analysis. Data obtained from the Pirouette software system summarizing PLS regression of KnowItAll-derived binned ^{1}H NMR data of BR extracts (independent variables) and TMA, FRAP, and DPPH (dependent variables) are shown in **Table 1**. For the test set, four PLS factors (components) were determined as optimum; standard error of prediction (SEP) or root mean squared error of prediction indicating goodness of fit and prediction residual error sum of squares (PRESS) each reached minimum values. Values of r and slope approaching 1 and intercept values approaching 0 were also indicators of goodness of fit. When test sets are compared, TMA values show the best fit with respect to SEP, PRESS, r, slope, and intercept parameters followed closely by FRAP values. Although DPPH test values are noteworthy with regard to fit, SEP and PRESS values are higher and the slope and intercept deviate more from the ideal compared to TMA and FRAP. These findings are consistent with the trends observed for the different assays (*28*) of these 19 BR extracts, where TMA and FRAP measurements were similar relative to each other ($r = 0.85$) but the relationships between these variables and DPPH values were substantially diminished ($r = 0.5$) or non-significant, respectively.

To determine relationships between compounds and TMA, FRAP, and DPPH, regression vectors (weighted sum of the loadings included in the model) were analyzed. As shown in **Figure 6**, when regression vector values were plotted against numbered bins (which corresponded to specific regions in the NMR spectra), TMA and FRAP showed responses that were often similar to each other yet different from DPPH. To determine how specific regions of the NMR spectra contributed to the variability, regression vector values were ranked. Structure assignments for specific constituents in the BR extracts could be made using binned data, and their impact was determined. Analysis of the top 100 positive vector values permitted rankings of compound contributions. Because the sugar region of the NMR spectrum of the BR extract was so complex, focus was placed on bins other than those from the 3.401−4.073 ppm region, where complicated overlapping patterns for many of the protons of attached saccharide moieties were observed. However, distinctive regions for anomeric (4.6−5.6 ppm) and xylosyl (3.00−3.24 ppm) protons were included. No bins had been collected in the solvent region around 3.31 ppm, and the bin at 3.97 ppm was excluded before the regression analysis, because we believe this strong singlet was a chemical artifact randomly introduced during sample processing and preliminary statistical analysis determined it as an outlier. In addition, bins in the top

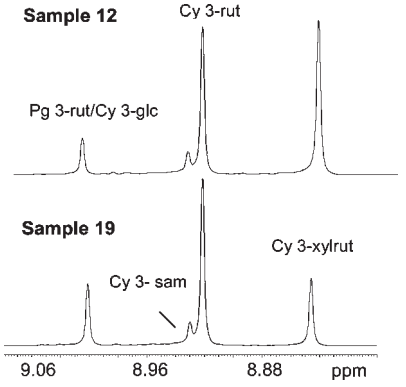

Figure 3. Selected region of the 750 MHz ^{1}H NMR spectra for samples 12 and 19.

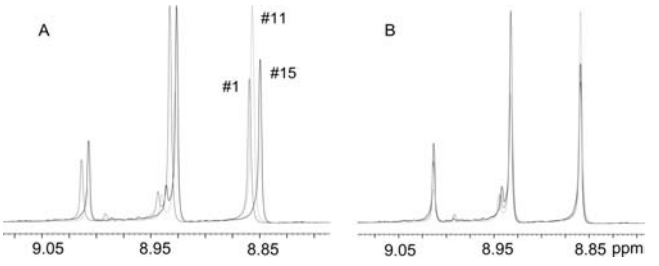

Figure 5. Selected regions of the ^{1}H NMR spectra showing (A) unaligned and (B) aligned spectra of BR samples 1, 11, and 15.

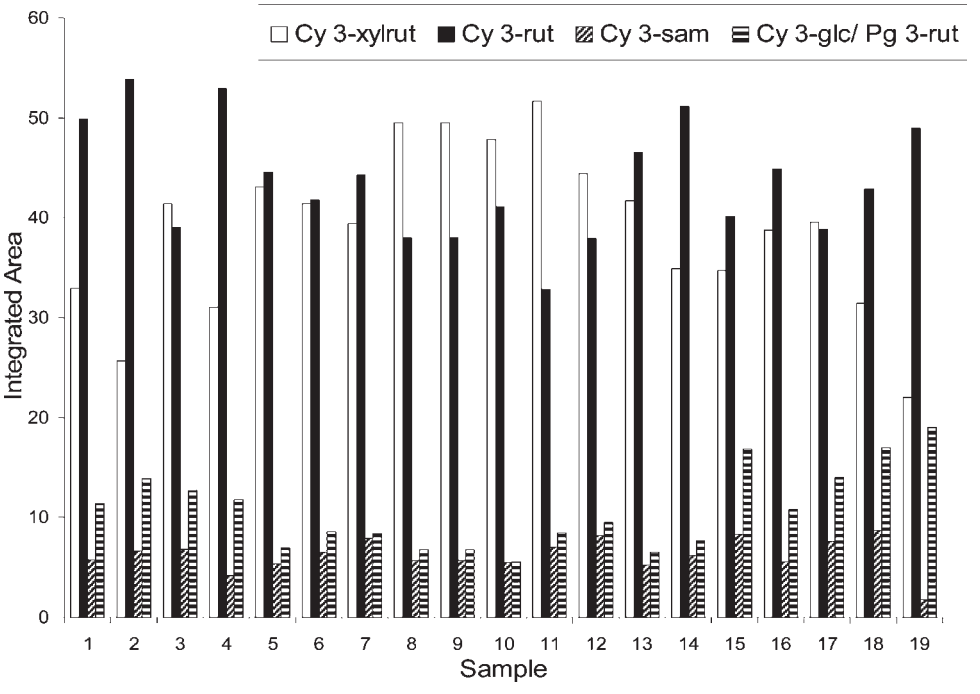

Figure 4. Integrated areas for the H4 region of the ^{1}H NMR spectra of 19 BR samples.

Table 1. PLS-Derived Summary of Fits

	TMA	FRAP	DPPH
SEP	0.04479	0.08173	0.18083
PRESS	0.03811	0.12692	0.62125
r	0.99999	0.99996	0.99800
slope	0.99978	1.00061	0.98783
intercept	0.00616	−0.02946	0.35733

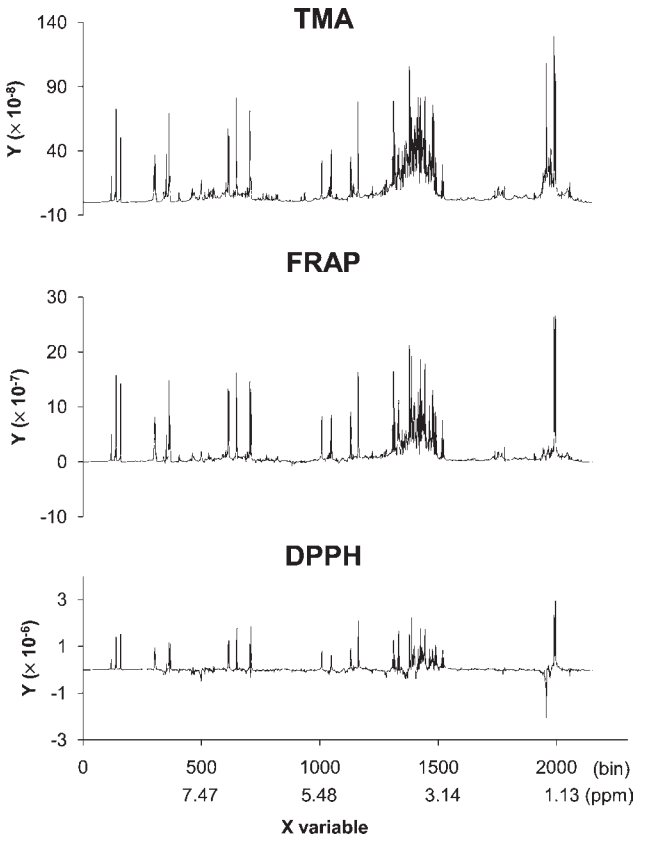

Figure 6. PLS regression vectors for TMA, FRAP, and DPPH versus bin number and chemical-shift (ppm) values.

100 corresponding to the 1.282−1.290 ppm region were not considered significant because 2D NMR analysis yielded their assignment as resonances of long-chain hydrocarbons attributed to leaching of column-coating material. Because most of the spectrum was analyzed and anthocyanins are associated with numerous resonances in distinctive regions of the spectrum, a number of peaks pertained to the same compound.

For example, **Figure 7** shows selected high-ranking regions and their assignments in the NMR spectrum of BR extract sample 19, which can be related to statistically important bins. According to the PLS analysis, many of the same bins were found in the top 100 regression vector values for TMA, FRAP, and DPPH but their rankings often differed. For example, the top two ranked bins for all three assays were attributed to the protons of the methyl resonances in Cy 3-rut (6‴) and/or Cy 3-xylrut (6^{IV}), which can be observed as distinctive doublets in the 1.1−1.4 ppm region of the NMR spectrum (**Figure 7**). The predominant ranking of these two bins was expected because Cy 3-rut and Cy 3-xylrut have been shown to be the most potent phenolic antioxidants in BRs (*25*). However, bins for the Cy 3-rut (6‴) doublet were ranked first and second for TMA, second and fourth for FRAP, and third and fifth for DPPH. Bins for the Cy 3-xylrut (6^{IV}) doublet were ranked fifth and sixth for TMA, first and third for FRAP, and first and second for DPPH. These results indicated

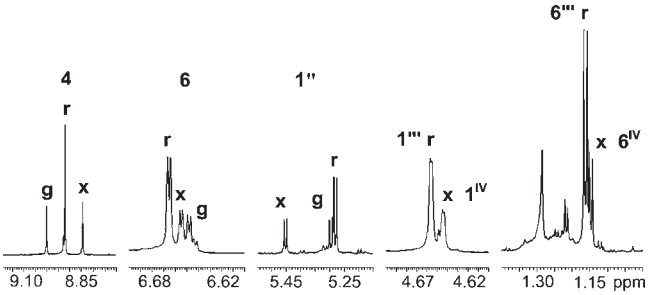

Figure 7. Regions of the ^{1}H 750 MHz NMR spectrum of BR extract sample 19 showing assigned resonances that correspond to high-ranking bins, where g = cyanidin 3-glucoside, r = cyanidin 3-rutinoside, and x = cyanidin 3-xylosylrutinoside.

that the amounts of Cy 3-rut in the samples were more significant than Cy 3-xylrut for TMA. As shown in **Table 2**, for FRAP, the regression vector values for Cy 3-xylrut (6^{IV}) and Cy 3-rut (6‴) bins were very close numerically, while Cy 3-xylrut (6^{IV}) was more significant than Cy 3-rut (6‴) for DPPH.

Differences in bin rankings also varied among assays for regression vectors corresponding to the anomeric protons of rhamnose. For TMA, Cy 3-rut (1‴) ranked 14th versus 94th for Cy 3-xylrut (1^{IV}). However, for FRAP, Cy 3-rut (1‴) ranked higher (11th) than Cy 3-xylrut (1^{IV}) (14th). Once again, for DPPH, Cy 3-xylrut (6th) ranked higher than Cy 3-rut (15th). In addition, the protons corresponding to position 4 on the cyanidin moieties behaved in a similar manner as the rhamnosyl anomeric protons. For TMA, Cy 3-rut ranked 18th versus 45th for Cy 3-xylrut, and for FRAP, Cy 3-rut ranked 13th versus 17th for Cy 3-xylrut, while Cy 3-xylrut is ranked higher (12th) than Cy 3-rut (16th) for DPPH.

For TMA, no bins corresponding to Cy 3-glc are ranked in the top 100. However, for FRAP and DPPH, proton 6 on cyanidin of the glucoside is ranked 22nd and 7th, respectively. In addition, proton 4 of Cy 3-glc is ranked 87th for DPPH but is not found in the top 100 rankings for TMA or FRAP. However, bins for protons 6 and 4 of Cy 3-glc are ranked as 245th and 203rd for TMA, which suggests that, even though Cy 3-glc was found in smaller quantities compared to Cy 3-rut and Cy 3-xylrut in the BR extracts, it contributed to all three assay results but was more significant for DPPH than for FRAP and less significant for TMA.

Advanced NMR Techniques. Multi-dimensional NMR analysis was also used to verify peak assignments of known bioactive compounds and to identify additional peaks that do not correspond to these known metabolites. When the regression vectors of two bins corresponding to 1.216 and 1.223 ppm were identified as important for TMA (**Table 2**), HSQC and HMBC experiments were employed to identify the structures responsible for these resonances. In the 1D ^{1}H NMR spectra for sample 19, these peaks were observed as a doublet downfield from the methyl doublets for Cy 3-rut and Cy 3-xylrut and the HSQC spectrum showed carbon shifts of 17.744 and 17.831 ppm, which were consistent with methyl carbons yet distinct from the methyl carbon shifts of Cy 3-rut and Cy 3-xylrut. The HMBC spectrum also revealed evidence of additional saccharide (C−H) correlations for a rhamnose attached to the 6″ carbon (H1‴/C6″, 4.744/67.745) of the glucosyl moiety. Because no correlations were observed in the 80 ppm region along δ^1H = 4.744 ppm, the presence of a xylosyl or another glucosyl moiety attached at the 2″ position of glucose was not indicated. Therefore, this unknown compound is tentatively assigned as a rutinoside with spectral properties that are distinct from but similar to Cy 3-rut.

Table 2. Selected Bins Showing NMR Ranges, Assignments, and Ranking of Regression Vector Values from PLS Regression Analysis of NMR Data versus Assays of TMA, FRAP, and DPPH

						regression vector values					
						TMA		FRAP		DPPH	
bin	bin range (ppm)		group	number	species	rank	value ($\times10^{-8}$)	rank	value ($\times10^{-7}$)	rank	value ($\times10^{-6}$)
1990	1.1677	1.1619	CH_3	$6'''$	Cy 3-rut	1	129.33	2	26.38	3	2.35
1993	1.1576	1.1535	CH_3	$6'''$	Cy 3-rut	2	113.96	4	24.14	5	2.25
1995	1.1513	1.1462	CH_3	6^{IV}	Cy- xylrut	5	100.38	1	26.73	1	2.98
1997	1.1441	1.1384	CH_3	6^{IV}	Cy- xylrut	6	94.46	3	26.00	2	2.93
1977	1.2158	1.2111	CH_3		unknown rut.	75	41.39	249	2.15	2057	−0.12
1975	1.2228	1.2187	CH_3		unknown rut.	72	41.94	300	1.71	2126	−0.26
1164	4.6419	4.6361	CH	1^{IV}	Cy 3-xylrut	94	37.46	14	15.51	6	2.10
1163	4.6460	4.6419	CH	1^{IV}	Cy 3-xylrut	92	37.80	128	4.59	201	0.14
1161	4.6558	4.6501	CH	$1'''$	Cy 3-rut	14	78.35	11	16.42	15	1.42
1132	4.7685	4.7630	CH	$1'''$	Cy 3-xylrut	103	35.50	49	8.69	40	0.84
1130	4.7785	4.7726	CH	$1'''$	Cy 3-xylrut	109	34.65	46	9.11	32	0.93
1050	5.2807	5.2749	CH	$1''$	Cy 3-rut	78	41.01	52	8.55	60	0.63
1048	5.2889	5.2848	CH	$1''$	Cy 3-rut	96	37.45	59	7.89	62	0.61
1008	5.4483	5.4425	CH	$1''$	Cy 3-xylrut	116	32.98	53	8.45	43	0.82
1006	5.4573	5.4524	CH	$1''$	Cy 3-xylrut	129	30.30	63	7.57	49	0.71
709	6.6568	6.6515	CH	6	Cy 3-glc	245	17.44	22	13.08	7	1.89
704	6.6718	6.6664	CH	6	Cy 3-rut	19	71.37	16	14.61	23	1.11
650	6.8787	6.8729	CH	8	Cy 3-xylrut	145	27.07	28	11.62	8	1.79
647	6.8901	6.8850	CH	8	Cy 3-rut	11	80.89	12	16.22	17	1.27
615	7.0166	7.0125	CH	$5'$	Cy 3-rut	52	48.01	32	10.83	30	0.96
612	7.0284	7.0243	CH	$5'$	Cy 3-rut	57	46.01	42	9.26	50	0.71
368	8.0114	8.0069	CH	$2'$	Cy 3-xylrut	1668	1.29	93	5.83	22	1.11
367	8.0155	8.0114	CH	$2'$	Cy 3-xylrut	212	20.31	76	6.83	35	0.90
363	8.0317	8.0260	CH	$2'$	Cy 3-rut	20	69.69	15	14.87	21	1.16
302	8.2753	8.2712	CH	$6'$	Cy 3-xylrut	101	35.94	56	8.21	31	0.95
301	8.2794	8.2753	CH	$6'$	Cy 3-rut	99	37.06	68	7.35	89	0.45
158	8.8614	8.8561	CH	4	Cy 3-xylrut	45	50.85	17	14.33	12	1.53
139	8.9350	8.9294	CH	4	Cy 3-rut	18	72.89	13	15.85	16	1.41
118	9.0169	9.0114	CH	4	Cy 3-glc	203	20.87	112	5.08	87	0.47

Structure−Activity Relationships. When results from antioxidant capacity assays are compared to the regression vectors of our model, structure−activity relationships should be considered. Previous research has shown that the structure of various components found in natural products can affect assay outcomes. For example, studies (*40*, *41*) have shown that the number and placement of hydroxyl groups of phenolics and polyphenolics can affect assay measurements for DPPH. In addition, the number and placement of attached saccharide moieties on glycosidic compounds can also influence assay results. Antioxidant measurements of anthocyanidins and their glycosides have yielded a wide range of results depending upon the assay used. One evaluation of anthocyanins (*42*) found that the activity decreased from the aglycone (cyanidin) > Cy 3-glc > Cy 3-rut > Cy 3-glucosylrutinoside. In another study (*43*), the antioxidant assay indicated higher values for Cy 3-rut as compared to Cy 3-glucosylrutinoside, leading them to conclude that a decrease in attached sugars led to an increase in antioxidant capacity. Research in our group (*25*) has also shown sugar moieties and their placement to be important factors in antioxidant capacity assays but indicated a different order of reactivity (i.e., Cy 3-rut > Cy 3-glc). These discrepancies suggest that structure−activity relationships applicable in one type of assay may not pertain to other assays based on different chemical reactions and methods of detection. The studies by Wang et al. (*42*) and Seeram et al. (*43*) employed similar assays based on the oxidation of phospholipids or liposome reactants as detected by fluorescence spectroscopy, whereas our study (*25*) measured the reactivity of purified anthocyanins with ferric ion or the DPPH radical as oxidants.

In addition, our study (*25*) reported Cy 3-glc antioxidant capacities determined by DPPH to be nearly 80% greater than those estimated from FRAP assays, whereas FRAP antioxidant values for Cy 3-rut exceed those measured by DPPH by approximately 14%. These structure−activity differences were consistent with our model, where Cy 3-glc is shown to be a more significant contributor to DPPH than to FRAP values.

Our model also suggested Cy 3-xylrut levels to be the topmost contributors to the variability in FRAP values, but Cy 3-rut contents were a very close second. In some cases (i.e., the anomeric proton on rhamnose), Cy 3-rut ($1'''$) ranked higher than Cy 3-xylrut (1^{IV}). The importance of Cy 3-rut in our model was consistent with its relatively strong reactivity in both DPPH and FRAP antioxidant assays in the previous study (*25*). However, our model predicted that Cy 3-xylrut is a more significant contributor to the variability in the DPPH results than Cy 3-rut. This suggests that, in mixtures with highly variable anthocyanin contents, Cy 3-xylrut may play a more important role in the kinetics of the DPPH assay than is readily apparent for the purified fractions. Complex mixtures of cyanidin-based anthocyanins in fruit and vegetable extracts were previously shown to be highly interactive in oxygen radical absorbance capacity (ORAC) assays, yielding results that were 3−5-fold greater than those expected from the concentrations and reactive strengths of their individual constituents (*44*). Moreover, in a study of free-radical-scavenging properties of lignans (*45*), the reaction mechanisms and kinetics of the DPPH radical were found to be complex and highly dependent upon the concentration of the reactants.

In conclusion, this investigation demonstrated that high-field ^{1}H NMR data obtained from BR extracts can be combined with multivariate statistical analysis to build a model using TMA and antioxidant capacity data from FRAP and DPPH assays.

This model yielded rankings of regression vectors for specific peak regions in the NMR spectra allowing for relationships to be established between individual components, especially the anthocyanins, Cy 3-rut, Cy 3-xylrut, and Cy 3-glc, and showed how they varied in importance depending upon the assay method. Our modeling process proved to be highly sensitive. Not only did it identify anthocyanins as major drivers of TMA and antioxidant assay responses and characterize the relationships between these assays, but it also provided a plausible explanation as to the variation in assay response with regards to specific phenolic compounds. The specificity and strength of the process to identify key NMR signals associated with specific compounds suggest that our approach might also be employed to determine relationships among bioactive components in natural products with *in vitro* or *in vivo* test results. Moreover, our metabolomics approach may also have a broad application for identifying and illustrating synergistic relationships among chemical constituents and bioactivity in any assay system where continuous biological data are acquired.

ACKNOWLEDGMENT

The authors thank Dr. Terrence Green of Lorain Community College, for his insights and assistance during the initial planning for these experiments. We also appreciate the efforts of Bert Bishop, Department of Information Technology, The Ohio State University, Ohio Agricultural Research and Development Center, for providing statistical consultation.

Supporting Information Available: Supplementary tables containing 750 MHz NMR data and supplementary figures showing $^{1}H/^{13}C$ multiple-bond correlations. HMBC, HSQC, and ^{1}H NMR data for a mixture (sample 19) from BR showing $^{1}H/^{13}C$ chemical-shift data for Cy 3-rut, Cy 3-xylrut, and Cy 3-glc (Supplementary Tables 1, 2, and 3), respectively, as well as 1D ^{1}H NMR data from a corresponding pure fraction of Cy 3-rut, Cy 3-xylrut, and Cy 3-glc. $^{1}H/^{13}C$ chemical-shift data for Cy 3-sam from HMBC, HSQC, and ^{1}H NMR spectra of a pure fraction (an authentic sample) (Supplementary Table 4). This material is available free of charge via the Internet at http://pubs.acs.org.

LITERATURE CITED

(1) Murch, S. J.; Rupasinghe, H. P. V.; Goodenowe, D.; Saxena, P. K. A metabolomic analysis of medicinal diversity in Huang-qin (*Scutellaria baicalensis* Georgi) genotypes: Discovery of novel compounds. *Plant Cell Rep*. **2004**, *23*, 419–425.

(2) Kite, G. C.; Howes, M.-J. R.; Simmonds, M. S. J. Metabolomic analysis of saponins in crude extracts of *Quillaja saponaria* by liquid chromatograph/mass spectrometry for product authentication. *Rapid Commun. Mass Spectrom*. **2004**, *18*, 2859–2870.

(3) Cho, S. K.; Yang, S.-O.; Kim, S.-H.; Kim, H.; Ko, J. S.; Riu, K. Z.; Lee, H.-Y.; Choi, H.-K. Classification and prediction of free-radical scavenging activities of dangyuja (*Citrus grandis* Osbeck) fruit extracts using ^{1}H NMR spectroscopy and multivariate statistical analysis. *J. Pharm. Biomed. Anal*. **2009**, *49*, 567–571.

(4) Son, H.-S.; Hwang, G.-S.; Kim, K. M.; Ahn, H.-J.; Park, W.-M.; van den Berg, F.; Hong, Y.-S.; Lee, C.-H. Metabolomic studies on geographical grapes and their wines using ^{1}H NMR analysis coupled with multivariate statistics. *J. Agric. Food Chem*. **2009**, *57*, 1481–1490.

(5) Son, H.-S.; Kim, K. M.; van den Berg, F.; Hwang, G.-S.; Park, W.-M.; Lee, C.-H.; Hong, Y.-S. ^{1}H nuclear magnetic resonance-based metabolomic characterization of wines by grape varieties and production areas. *J. Agric. Food Chem*. **2008**, *56*, 8007–8016.

(6) Abdel-Farid, I. B.; Jahangir, M.; van den Hondel, C. A. M. J. J.; Kim, H. K.; Choi, Y. H.; Verpoorte, R. Fungal infection-induced metabolites in *Brassica rapa*. *Plant Sci*. **2009**, *176*, 608–615.

(7) Bodenhausen, G.; Ruben, D. J. Natural abundance nitrogen-15 NMR by enhanced heteronuclear spectroscopy. *J. Chem Phys. Lett*. **1980**, *69*, 185–189.

(8) Bax, A.; Summers, M. F. Proton and carbon-13 assignments from sensitivity-enhanced detection of heteronuclear multiple-bond connectivity by 2D multiple quantum NMR. *J. Am. Chem. Soc*. **1986**, *108* (8), 2093–2094.

(9) Han, C.; Ding, H.; Casto, B.; Stoner, G. D.; D'Ambrosio, S. M. Inhibition of the growth of premalignant and malignant human oral cell lines by extracts and components of black raspberries. *Nutr. Cancer* **2005**, *51* (2), 207–217.

(10) Reen, R. K.; Nines, R.; Stoner, G. D. Modulation of *N*-nitrosomethylbenzylamine metabolism by black raspberries in the esophagus and liver of Fischer 344 rats. *Nutr. Cancer* **2006**, *54* (1), 47–57.

(11) Kresty, L. A.; Frankel, W. L.; Hammond, C. D.; Baird, M. E.; Mele, J. M.; Stoner, G. D.; Fromkes, J. J. Transitioning from preclinical to clinical chemopreventive assessments of lyophilized black raspberries: Interim results show berries modulate markers of oxidative stress in Barrett's esophagus patients. *Nutr. Cancer* **2006**, *54*, 148–156.

(12) Harris, G. K.; Gupta, A.; Nines, R. G.; Kresty, L. A.; Habib, S. G.; Frankel, W. L.; LaPerle, K.; Gallaher, D. D.; Schwartz, S. J.; Stoner, G. D. Effects of lyophilized black raspberries on azoxymethane-induced colon cancer and 8-hydroxy-2′-deoxyguanosine levels in the Fischer 344 rat. *Nutr. Cancer* **2001**, *40* (2), 125–133.

(13) Rodrigo, K. A.; Rawal, Y.; Renner, R. J.; Schwartz, S. J.; Tian, Q.; Larsen, P. E.; Mallery, S. R. Suppression of the tumorigenic phenotype in human oral squamous cell carcinoma cells by an ethanol extract derived from freeze-dried black raspberries. *Nutr. Cancer* **2006**, *54*, 58–68.

(14) Stoner, G. D.; Wang, L. S.; Zikri, N.; Chen, T.; Hecht, S. S.; Huang, C.; Sardo, C.; Lechner, J. F. Cancer prevention with freeze-dried berries and berry components. *Semin. Cancer Biol*. **2007**, *17*, 403–410.

(15) Hecht, S. S.; Huang, C.; Stoner, G. D.; Li, J.; Kenney, P. M. J.; Sturla, S. J.; Carmella, S. G. Identification of cyanidin glycosides as constituents of freeze-dried black raspberries which inhibit anti-benzo[*a*]pyrene-7,8-diol-9,10-epoxide induced NFkB and AP-1 activity. *Carcinogenesis* **2006**, *27*, 1617–1626.

(16) Stoner, G. D.; Chen, T.; Kresty, L. A.; Aziz, R. M.; Reinemann, T.; Nines, R. Protection against esophageal cancer in rodents with lyophilized berries: Potential mechanisms. *Nutr. Cancer* **2006**, *54*, 33–46.

(17) Stoner, G. D.; Dombkowski, A. A.; Reen, R. K.; Cukovic, D.; Salagrama, S.; Wang, L.-S.; Lechner, J. F. Carcinogen-altered genes in rat esophagus positively modulated to normal levels of expression by both black raspberries and phenylethyl isothiocyanate. *Cancer Res*. **2008**, *68*, 6460–6467.

(18) Mumper, R. J.; Mallery, S. R.; Stoner, G. D.; Larsen, P. E. Mucoadhesive gels containing berry preparations and extracts for oral cancer chemoprevention. PCT Int. Appl. WO, University of Kentucky Research Foundation and The Ohio State University Research Foundation, **2008**; p 37.

(19) Mallery, S. R.; Zwick, J. C.; Pei, P.; Tong, M.; Larsen, P. E.; Shumway, B. S.; Lu, B.; Fields, H. W.; Mumper, R. J.; Stoner, G. D. Topical application of a bioadhesive black raspberry gel modulates gene expression and reduces cyclooxygenase 2 protein in human premalignant oral lesions. *Cancer Res*. **2008**, *68*, 4945–4957.

(20) Li, J.; Zhang, D.; Stoner, G. D.; Huang, C. Differential effects of black raspberry and strawberry extracts on BaPDE-induced activation of transcription factors and their target genes. *Mol. Carcinog*. **2008**, *47*, 286–294.

(21) Seeram, N. P. Berry fruits for cancer prevention: Current status and future prospects. *J. Agric. Food Chem*. **2008**, *56*, 630–635.

(22) Chen, T.; Rose, M. E.; Hwang, H.; Nines, R. G.; Stoner, G. D. Black raspberries inhibit *N*-nitrosomethylbenzylamine (NMBA)-induced angiogenesis in rat esophagus parallel to the suppression of COX-2 and iNOS. *Carcinogenesis* **2006**, *27*, 2301–2307.

(23) Jung, J.; Son, M.-Y.; Jung, S.; Nam, P.; Sung, J.-S.; Lee, S.-J.; Lee, K.-G. Antioxidant properties of Korean black raspberry wines and

their apoptotic effects on cancer cells. *J. Sci. Food Agric.* **2009**, *89*, 970–977.
(24) Ozgen, M.; Reese, R. N.; Tulio, A. Z., Jr.; Scheerens, J. C.; Miller, A. R. Modified 2,2-azino-bis-3-ethylbenzothiazoline-6-sulfonic acid (ABTS) method to measure antioxidant capacity of selected small fruits and comparison to ferric reducing antioxidant power (FRAP) and 2,2′-diphenyl-1-picrylhydrazyl (DPPH) methods. *J. Agric. Food Chem.* **2006**, *54*, 1151–1157.
(25) Tulio, A. Z., Jr.; Reese, R. N.; Wyzgoski, F. J.; Rinaldi, P. L.; Fu, R.; Scheerens, J. C.; Miller, A. R. Cyanidin 3-rutinoside and cyanidin 3-xylosylrutinoside as primary phenolic antioxidants in black raspberry. *J. Agric. Food Chem.* **2008**, *56*, 1880–1888.
(26) Tulio, A. Z., Jr.; Ozgen, M.; Reese, R. N.; Miller, A. R.; Scheerens, J. C. Cyanidin 3-rutinoside levels and antioxidant properties in black raspberries as impacted by fruit maturation and storage temperature. *HortScience* **2007**, *42*, 985.
(27) Ozgen, M.; Tulio, A. Z., Jr.; Chanon, A. M.; Janakiraman, N.; Reese, R. N.; Miller, A. R.; Scheerens, J. C. Phytonutrient accumulation and antioxidant capacity at eight developmental stages of black raspberry fruit. *HortScience* **2006**, *41*, 1082.
(28) Ozgen, M.; Wyzgoski, F. J.; Tulio, A. Z., Jr.; Gazula, A.; Miller, A. R.; Scheerens, J. C.; Reese, R. N.; Wright, S. R. Antioxidant capacity and phenolic antioxidants of midwestern black raspberries grown for direct markets are influenzed by production site. *HortScience* **2008**, *43* (7), 2039–2047.
(29) Giusti, M. M.; Wrolstad, R. E. Characterization and measurement of anthocyanins by UV−visible spectroscopy. In *Handbook of Food Analytical Chemistry: Pigments, Colorants, Flavors, Texture, and Bioactive Food Components*; Wrolstad, R. E., Schwartz, S. J., Eds.; Wiley: New York, 2005; pp 19−31.
(30) Benzie, I. F. F.; Strain, J. J. The ferric reducing ability of plasma (FRAP) as a measure of "antioxidant power": The FRAP assay. *Anal. Biochem.* **1996**, *239*, 70–76.
(31) Brand-Williams, W.; Cuvelier, M. E.; Berset, C. Use of a free radical method to evaluate antioxidant activity. *Lebensm.-Wiss. Technol.* **1995**, *28*, 25–30.
(32) Singleton, V. L.; Orthofer, R.; Lamuela-Raventós, R. M. Analysis of total phenols and other oxidation substrates and antioxidants by means of Folin−Ciocalteu reagent. *Methods Enzymol.* **1999**, *299*, 152–178.
(33) Lohachoompol, V.; Srzednicki, G.; Craske, J. The change of total anthocyanins in blueberries and their antioxidant effect after drying and freezing. *J. Biomed. Biotechnol.* **2004**, *5*, 248–252.
(34) Kupce, E.; Freeman, R. Stretched adiabatic pulses for broadband spin inversion. *J. Magn. Reson., Ser. A* **1995**, *117*, 246–256.
(35) States, D. J.; Haberkorn, R. A.; Ruben, D. J. A two-dimensional nuclear overhauser experiment with pure absorption phase in 4 quadrants. *J. Magn. Reson.* **1982**, *48*, 286.
(36) Tian, Q.; Giusti, M. M.; Stoner, G. D.; Schwartz, S. J. Characterization of a new anthocyanin in black raspberries (*Rubus occidentalis*) by liquid chromatography electrospray ionization tandem mass spectrometry. *Food Chem.* **2006**, *94*, 465–468.
(37) Cabrita, L.; Andersen, O. M. Anthocyanins in blue berries of *Vaccinium padifolium*. *Phytochemistry* **1999**, *52*, 1693–1696.
(38) Cabrita, L.; Froystein, N. A.; Andersen, O. M. Anthocyanin trisaccharides in blue berries of *Vaccinium padifolium*. *Food Chem.* **2000**, *69*, 33–36.
(39) Westerhuis, J. A.; de Jong, S.; Smilde, A. K. Direct othogonal signal correction. *Chemom. Intell. Lab. Syst.* **2001**, *56*, 13–25.
(40) Butkovic, V.; Klasinc, L.; Bors, W. Kinetic study of flavonoid reactions with stable radicals. *J. Agric. Food Chem.* **2004**, *52*, 2816–2820.
(41) Thavasi, V.; Bettens, R. P. A.; Leong, L. P. Temperature and solvent effects on radical scavenging ability of phenols. *J. Phys. Chem. A* **2009**, *113*, 3068–3077.
(42) Wang, H.; Nair, M. G.; Strasburg, G. M.; Chang, Y. C.; Booren, A. M.; Gray, J. I.; DeWitt, D. L. Antioxidant and antiinflammatory activities of anthocyanins and their aglycon, cyanidin, from tart cherries. *J. Nat. Prod.* **1999**, *62*, 294–296.
(43) Seeram, N. P.; Momin, R. A.; Nair, M. G.; Bourquin, L. D. Cyclooxygenase inhibitory and antioxidant cyanidin glycosides in cherries and berries. *Phytomedicine* **2001**, *8*, 362–369.
(44) Stintzing, F. C.; Stintzing, A. S.; Carle, R.; Frei, B.; Wrolstad, R. E. Color and antioxidant properties of cyanidin-based anthocyanin pigments. *J. Agric. Food Chem.* **2002**, *50*, 6172–6181.
(45) Eklund, P. C.; Langvik, O. K.; Warna, J. P.; Salmi, T. O.; Willfor, S. M.; Sjoholm, R. E. Chemical studies on antioxidant mechanisms and free radical scavenging properties of lignans. *Org. Biomol. Chem.* **2005**, *3*, 3336–3347.

Received for review December 13, 2009. Revised manuscript received February 14, 2010. Accepted February 17, 2010. We thank the Kresge Foundation and the donors to the Kresge Challenge Program at the University of Akron for funds used to purchase the 750 MHz NMR instrument used in this work. Salaries and research support are provided in part by state and federal funds appropriated to the The Ohio State University, Ohio Agricultural Research and Development Center, U.S. Department of Agriculture Special Research Grants for Dietary Intervention 2003-34501-13965 and 2005-38903-02313.